Enhanced magnetization drift velocity and current polarization in $(CoFe)_{1-x}Ge_x$ alloys

M. Zhu,[1, 2, *] B. D. Soe,[1, 3] R. D. McMichael,[1, †] M. J. Carey,[4] S. Maat,[4] and J. R. Childress[4]

[1]*Center for Nanoscale Science and Technology, National Institute*
of Standards and Technology, Gaithersburg, Maryland 20899, USA
[2]*Maryland Nanocenter, University of Maryland, College Park, Maryland 20742, USA*
[3]*Department of Engineering, Harvey Mudd College, Claremont, California 91711, USA*
[4]*San Jose Research Center, Hitachi Global Storage Technologies, San Jose, California 95135, USA*
(Dated: February 17, 2011)

A spin wave Doppler technique is used to measure the drift velocity of the magnetization in current-carrying $(CoFe)_{1-x}Ge_x$ alloys. For a current density of 10^{11} A/m², we obtain a large enhancement of drift velocity with increased Ge concentration from 3.1±0.2 m/s for CoFe to 8.2±0.6 m/s for $(CoFe)_{0.7}Ge_{0.3}$. Interpretation of these values yields current polarization increasing from 0.84 ± 0.04 to 0.95 ± 0.05 as the Ge doping increases. While both spin dependent conductivities decrease with increasing Ge concentration, the maximum in polarization is associated with a stronger relative change in the minority spin conductivity. Publ. Applied Physics Letters, **98**, 072510 (2011).

PACS numbers:

The implementation of magnetic tunnel junction (MTJ) based read head sensors has greatly improved the areal density of modern hard disk drives due to their large tunneling magnetoresistance (TMR). However, the inherent high resistance-area (RA) product of the tunnel junctions imposes large noise, decreased sensor bandwidth and limitations in fabrication processes when the sensor lateral dimension is scaled below 50 nm [1]. On the other hand, metallic current-perpendicular-to-the-plane (CPP) giant magnetoresistance (GMR) spin valves have much lower RA product with good scalability, and as a result, offer lower noise and higher bandwidth [2]. The main challenge for CPP spin valves, however, lies in its lower GMR ratio relative to TMR, resulting in poor sensitivity. The CPP-GMR ratio is determined by the asymmetrical spin scattering in the bulk ferromagnetic films and at the interface between ferromagnetic and non-ferromagnetic layers [3]. In bulk transport, this spin-scattering asymmetry is manifested as the spin polarization of the current: $P = (\sigma_\uparrow - \sigma_\downarrow)/(\sigma_\uparrow + \sigma_\downarrow)$, where $\sigma_{\uparrow(\downarrow)}$ is the conductivity of spin up(down) electrons. Thus, materials with a higher current spin polarization are promising for achieving higher GMR values.

One class of the extensively studied highly-spin-polarized materials is the Heusler alloys, such as $Co_2FeAl_{0.5}Si_{0.5}$ [4] and Co_2MnSi [5], which exhibit very high GMR values. However, a high polarization in Heusler alloys is only achieved in the ordered $L2_1$ structure, which is established by an annealing procedure over 400 °C [6]. This high-temperature process is incompatible with fabrication of the read head sensors.

In contrast to these full Heusler alloys, recently investigated $(CoFe)_{1-x}Ge_x$ alloys require a lower annealing temperature to form a high spin-polarization $B2$-
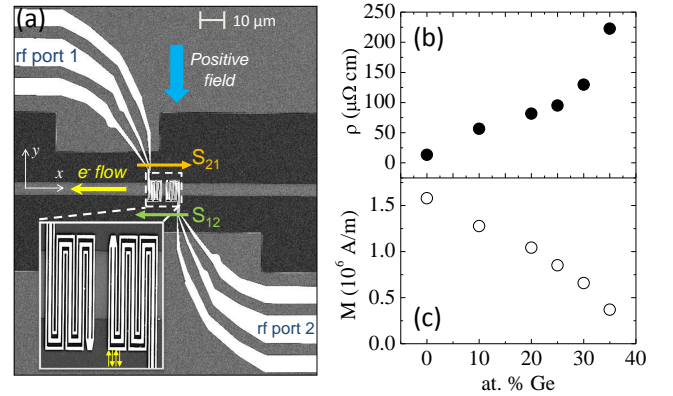
———
*Current Address: Seagate Technology, Bloomington MN 55435
†Electronic address: robert.mcmichael@nist.gov

FIG. 1: (Color online) (a) Scanning electron microscope (SEM) image of the fabricated $(CoFe)_{1-x}Ge_x$ device with 4 μm width. S_{12} (S_{21}) refers to the spin wave transmission from RF port 2(1) to port 1(2). Positive current represents that the electrons flow in the negative x direction. The inset shows the zoomed-in image of the microwave antennas.(b) Resistivity and (c) magnetization as a function of Ge concentration.

like chemically ordered structure where Ge atoms preferably occupy the center site in a bcc lattice [7]. A first-principles calculation of $(CoFe)_{0.75}Ge_{0.25}$ based on this structure shows a pseudogap in the minority spin band around the Fermi energy [7]. Moreover, observed high GMR values [8] have made $(CoFe)_{1-x}Ge_x$ a promising candidate for CPP spin valve electrodes. In this letter, we present measurements of current spin polarization, magnetization drift velocity and spin-dependent conductivities in $(CoFe)_{1-x}Ge_x$ alloys (x from 0 to 0.30), using a spin wave Doppler technique [9–11].

The $(CoFe)_{1-x}Ge_x$ thin films were co-sputtered from $Co_{50}Fe_{50}$ and Ge targets and patterned into wires with 2 μm or 4 μm width using photolithography and lift-off processes. The film stack consists of Ta(2)/ Ru(1)/ CoFe(0.6)/ $(CoFe)_{1-x}Ge_x$(30)/ CoFe(0.6)/ Ru(1)/ Ta(4)

(numbers indicate layer thickness in nm) on high-resistivity Si wafers. The Ge concentration x was varied from 0 to 0.35, and was verified by x-ray fluorescence using Co, Fe, and Ge standards to be within $\pm$ 0.02 uncertainty. The films were annealed in vacuum at 245 °C for 5 hours[8]. We then placed four dc contacts at the ends of the magnetic wires as current/voltage probes and covered the wires with a 80 nm Al_2O_3 as an insulating layer to separate them from microwave antennas that were patterned by E-beam lithography. A detailed description of the device fabrication is given elsewhere [11]. Fig.1(a) shows an example of the devices used in the spin wave Doppler experiment.

We connected the microwave antennas to the two ports of a vector network analyzer. The microwave antennas have periodic structures [inset of Fig.1(a)] which carry microwave current in alternating directions. The generated microwave fields couple to the spin wave modes primarily at two wave vectors $k_0 = 8.38$ μm^{-1} and $k_1 = 2.79$ μm^{-1}, determined by the structural periodicity of the antennas. Spin waves propagate over a distance D = 7 μm and are detected inductively by another antenna as a magnetic resonance of the transmission signal. In-plane static fields between 0.12 T and 0.18 T are applied perpendicular to the magnetic wires and all the measurements involve subtraction of background spectra at a reference field that shifts the resonance out of the measured frequency window [11].

The magnetization drift velocity, arising from adiabatic spin transfer between polarized electrons and local magnetization, is written as [12, 13],

$$\mathbf{v} = -\frac{g\mu_B P}{2M_s|e|}\mathbf{J}, \qquad (1)$$

where $g \approx 2$ is the Landé g-factor, P is the current spin polarization and $\mathbf{J}$ is the current density. For a fixed wave vector $\mathbf{k}$, the spin-wave dispersion $\omega(\mathbf{k})$ is shifted by an amount $\Delta\omega = \mathbf{k}\cdot\mathbf{v}$ when a polarized current flows in the magnetic wire [9, 14]. The sign of the frequency shift depends on the relative direction between electron flow and the spin wave propagation. From the current-dependent spin wave frequency shift, the magnitude and the direction of the drift velocity can be obtained as a function of current density.

In this experiment, the current density in the active magnetic layers is a critical parameter in determining the drift velocity and polarization. There are several factors that can affect the calculation of current density: (1) the shunt current carried by the capping and underlying metal layers; (2) the difference between actual device and nominal device widths; (3) the thickness of the magnetic films.

To account for the effect of current shunting, we measured the resistance of samples with the same Ge concentration, the same underlying and capping layers, but different magnetic layer thicknesses (15 nm, 30 nm, 50 nm). We used a parallel-conductor model to calculate the effective resistivity, (220±20) $\mu\Omega$ cm, of the underlying/capping layers. The current flowing in the magnetic layer is obtained by taking into consideration the resistivity ratio between the active layer and that of the underlying/capping layers, with corrected currents ranging from 98% to 85% of the injected current for CoFe and $(CoFe)_{0.70}Ge_{0.30}$, respectively.

We also determined the electrical width of the stripes by measuring the resistance of samples with different nominal widths. Plots of conductance vs. the designed width yield the difference between electrical width and the designed width, which is on the order of a few hundred nanometers. Heating effects were estimated by correlating measurements of resistance vs. temperature and resistance vs. current. A maximum temperature rise of 30 °C is estimated for the 25% Ge sample.

The thickness of the films was determined by x-ray reflectometry on calibration samples of similar thicknesses, with an uncertainty of less than 2 %. Interfacial roughness and interdiffusion effects may play a role in reducing the effective thickness of the magnetic films. Moreover, during the device fabrication, unintentional oxidation by oxygen plasma cleaning or annealing may also reduce the magnetic thin film thickness. In the calculation of current density, we therefore use the nominal thickness of 30 nm with an overall estimated uncertainty of 5 %. All the uncertainties reported in this Letter represent one standard deviation.

Similarly to what has been reported earlier[8], the resistivity of $(CoFe)_{1-x}Ge_x$ shows a monotonic increase as the Ge content increases [Fig.1(b)]. The values reported here are significantly larger than in ref. 8, and we speculate that improvements in processing, capping layers and measurements of thickness dependence may responsible for this difference. We also measured magnetization by vibrating sample magnetometry on separate control samples that were deposited and annealed with the patterned devices. The uncertainty of these measurements is about 3 %. As can be seen from Fig.1(c), the saturation magnetization is reduced as a result of Ge doping.

Examples of current-induced frequency shift Δf in a 2 μm wide stripe of $(CoFe)_{0.75}Ge_{0.25}$ in 0.18 T applied field are shown in Fig.2(a) . In the upper panel, Z_{12} and Z_{21} are shifted to higher and lower frequencies respectively at a positive current density of 1.4×10^{11} A/m^2, and in the lower panel, the sign of Δf changes when the current reverses. We determined Δf by cross-correlating the two transmission curves, yielding a measurement uncertainty of less than 2.5 MHz.

The inset of Fig.2(b) shows Δf for samples with different Ge content. Vertical offsets are artifacts of the method used to eliminate non-reciprocal effects[11]. The alloy with 35 % Ge shows a very weak resonance signal, which precludes frequency-shift measurements. From the frequency shift, the magnetization drift velocity is obtained from $v = \pi\Delta f/k$. We observe a dramatic enhancement of drift velocity v with increasing Ge concentration as indicated by the slope change of Δf vs. J. As shown in Fig.2, at a current density of 10^{11} A/m^2, the
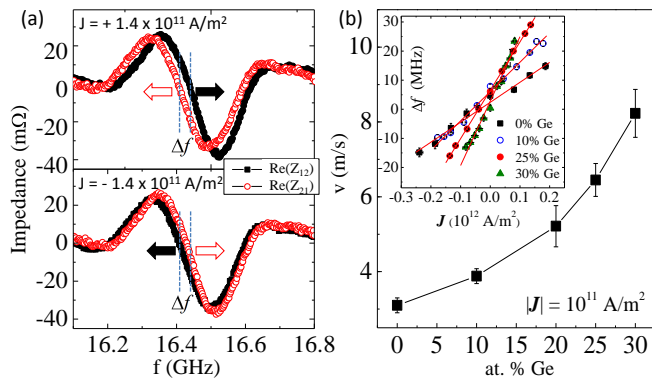
3

FIG. 2: (Color online) (a) Real part of the transmission impedance Z_{12} and Z_{21} extracted from S_{12} and S_{21} when a current density of $\pm 1.4 \times 10^{11}$ A/m^2 is applied in the (CoFe)$_{0.75}$Ge$_{0.25}$ wire. (b) Magnetization drift velocity as a function of Ge concentration for a current density of 10^{11} A/m^2. The inset shows the relative frequency shift Δf of transmission vs. current density for different (CoFe)$_{1-x}$Ge$_x$ alloys. Lines in the inset are linear fits.
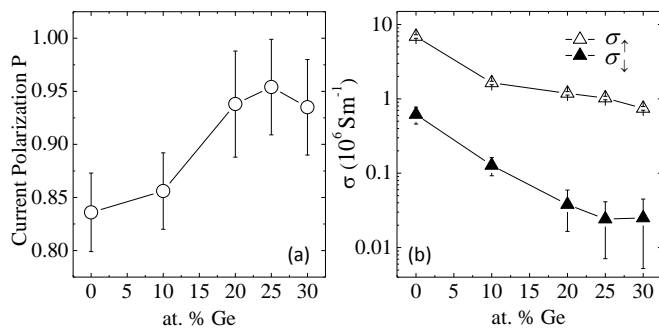

FIG. 3: (a) Spin polarization of (CoFe)$_{1-x}$Ge$_x$ alloys. (b) Changes of spin-up and spin-down conductivities with increasing Ge doping (y in log scale).

drift velocity increases from 3.1 ± 0.2 m/s for CoFe to 8.2 ± 0.6 m/s for (CoFe)$_{0.7}$Ge$_{0.30}$.

We extract polarization values from Eq.(1) using the slope of v vs. J and the magnetization data, and plot them in Fig.3(a). The current polarization increases sharply between 10 % and 20 %, and reaches a maxium

of 0.95 ± 0.04 near 25 % Ge. This polarization maximum is in concert with a magnetic damping minimum in (CoFe)$_{1-x}$Ge$_x$ [7] and a GMR maximum in CoFe$_{1-x}$Ge$_x$-based spin valves[8] at similar compositions. The polarization maximum is greater than the value of 0.71 ± 0.08 at 30 % Ge obtained from the free-layer thickness dependence of the resistivity in the spin valve structures[8]. The origins of this difference are not well-understood.

Compared to the behavior of P, v depends more strongly on Ge concentration (Fig. 2b), and it is clear that the strong increases in v arise primarily from decreasing M_s.

To further investigate the carrier transport, we separate spin-up and spin-down conductivity using: $\sigma_\uparrow = (1 + P)/2\rho$, and $\sigma_\downarrow = (1 - P)/2\rho$. The spin-dependent conductivities are plotted in Fig.3(b) on a logarithmic scale. Clearly, the two conductivities show distinct responses to the Ge doping at $x > 10$ %: the relative decrease for $\sigma_\downarrow$ is much stronger than that for $\sigma_\uparrow$. At 25 % Ge, $\sigma_\downarrow$ is almost completely suppressed with only 0.02 $\times 10^6$ S/m, which is 1/25 of its value in CoFe, whereas $\sigma_\uparrow$ only decreases by a factor of 1/6. The difference between the conductivity changes for the two spin channels is consistent with a reduced minority density of states [7] although spin-dependent electron velocities and relaxation times can play a dominant role in determining spin-dependent conductivity in CoFe alloys[15].

In summary, incorporating Ge into CoFe is found to increase the spin polarization in the bulk electron transport. The maximum polarization is achieved in the Ge composition range of 20 % to 30 %, which is in concert with the damping minimum in (CoFe)$_{1-x}$Ge$_x$ films[7] and the higher GMR values in the (CoFe)$_{1-x}$Ge$_x$-based spin valves with similar composition[8]. The enhanced magnetization drift velocity with Ge doping signifies stronger adiabatic spin transfer due to the reduction of magnetization and the increase of polarization.

[1] J. R. Childress and R. E. Fontana, Comptes Rendus Physique **6**, 997 (2005).
[2] J. R. Childress, M. J. Carey, S. Maat, N. Smith, R. E. Fontana, D. Druist, K. Carey, J. A. Katine, N. Robertson, T. D. Boone, M. Alex, J. Moore, and C. H. Tsang, IEEE Trans. Mag. **44**, 90 (2008).
[3] E. Y. Tsymbal and D. Pettifor (Academic Press, San Diego, 2001), vol. 56 of *Solid State Physics*, pp. 113 – 237.
[4] T. Furubayashi, K. Kodama, H. Sukegawa, Y. K. Taka-
hashi, K. Inomata, and K. Hono, Appl. Phys. Lett. **93**, 122507 (2008).
[5] K. Kodama, T. Furubayashi, H. Sukegawa, T. M. Nakatani, K. Inomata, and K. Hono, J. Appl. Phys. **105**, 07E905 (2009).
[6] T. Furubayashi, K. Kodama, T. M. Nakatani, H. Sukegawa, Y. K. Takahashi, K. Inomata, and K. Hono, J. Appl. Phys. **107**, 113917 (2010).
[7] H. Lee, Y.-H. A. Wang, C. K. A. Mewes, W. H. Butler, T. Mewes, S. Maat, B. York, M. J. Carey, and J. R.

Childress, Appl. Phys. Lett. **95**, 082502 (2009).

[8] S. Maat, M. J. Carey, and J. R. Childress, Appl. Phys. Lett. **93**, 143505 (2008).

[9] V. Vlaminck and M. Bailleul, Science **322**, 410 (2008).

[10] V. Vlaminck and M. Bailleul, Phys. Rev. B **81**, 014425 (2010).

[11] M. Zhu, C. L. Dennis, and R. D. McMichael, Phys. Rev. B **81**, 140407 (2010).

[12] S. Zhang and Z. Li, Phys. Rev. Lett. **93**, 127204 (2004).

[13] A. Thiaville, Y. Nakatani, J. Miltat, and Y. Suzuki, Europhys. Lett. **69**, 990 (2005).

[14] S.-M. Seo, K.-J. Lee, H. Yang, and T. Ono, Phys. Rev. Lett. **102**, 147202 (2009).

[15] Y. Kota, T. Takahashi, H. Tsuchiura, and A. Sakuma, J. Appl. Phys. **105**, 07B716 (2009).